Towards the optimal sizing of solar-powered pump-pipe-storage systems

Tawanda Hove[1], Emmanuel Mungofa[2]

[1] Lecturer, National University of Lesotho, Roma (Lesotho)

[2] Lecturer, University of Zimbabwe, Harare (Zimbabwe)

Abstract

In this paper, a method for optimal sizing and performance prediction of a solar pump-pipe-storage system is proposed. The solar-pumping-system components namely, the pump; solar photovoltaic array; pumping mains and the water storage are sized in an integrated approach. The method develops a flow-power function, which comprehensively takes into account the time-step variation of solar irradiance and its effect on the pump system flow-rate and total dynamic head. The flow-power function expresses the flow output of the solar pumping system as a function of the time-step variation of the photovoltaic array power output, for a given pump and pipe size. Especially for long pumping mains, the PV array power required to deliver a specified daily volume of water reduces significantly as the pumping main pipe diameter is increased. Depending on the relative specific costs of PV array and pipe, an economically optimum combination of these two system components, which delivers the desired daily volume of water at the least cost of pumping, can be arrived at. Applying a time-step balance of the hourly pump flow output with the hourly water demand, also enables a more exact estimation of the required balancing storage, through the mass-balance-curve approach. The method proves to be a significant improvement to the traditional simplified approach of sizing solar pumping systems. It can result in significantly reduced unit cost of pumping and reduced cost of storage. In the present case study, the required PV array power was reduced by 20% and the required water storage capacity reduced by 50% when compared to their respective values prescribed by the traditional sizing method.

Keywords: solar pumping systems, optimal sizing, dynamic variation, flow-power function, least cost of pumping

1. Introduction

With the advent of solar pump technology, it is now possible to use the sun‘s energy for pumping water for small-scale irrigation, sanitary water supply, live-stock watering and other applications, thereby displacing the need to use conventional electricity or diesel pumps and thereby improving livelihoods for communities living off-grid. Since the price of photovoltaic (PV) modules has reduced by 80% and that of petroleum fuel has increased by 250% in the past decade, Foster and Cota, 2014, solar pumps can now easily be more cost-effective than diesel/gasoline powered pumps- the conventional technology for off-grid water pumping. In addition, particularly for irrigation and live-stock watering applications, solar pumping has a natural synergy with water demand; there is more water demand during the sunny dry season when solar radiation for pumping water is also more available. Zimbabwe receives abundant sunshine (an annual average of 5.6 to 7.1 kWh/day), which is ubiquitously distributed over the country, Hove et al, 2014, yet 75 % of the rural population in not connected to the grid. The scenario described above situation makes the country (Zimbabwe) an ideal market for solar pumping.

A solar water pump system is a fairly simple structure and typically consists of a water pump (submersible or surface pump), control electronics (for protecting the pump and controlling speed of the pump), solar panels and water-conveyance pipes. Most solar water pump systems do not use expensive electro-chemical storage batteries but instead use water storage tanks for storing energy. However, the sizing and performance prediction of the solar pump-pipe system is a not-so-straightforward exercise, since the stochastic behaviour of the PV-energy-driving weather elements (the solar radiation and ambient temperature) as well as the specific empirical response of pump-pipe system performance to changes of these elements need to be expertly managed. Several simulation programs have been developed by researchers for the performance prediction of the PV water pumping system based on solar radiation data of a location which are found to be sufficiently accurate in evaluating the actual performance of solar pumps.

Selection and/or peer review under responsibility of Scientific Committee
doi:10.18086/swc.2019.34.02 Available at http://proceedings.ises.org

These combined with optimization sizing techniques developed have resulted in the selection of various components and refinement of PV pumping technology by the manufacturers (Chandel et al, 2015).

In this study another solar water pumping system optimization method is proposed. The method is based on developing flow-power functions from the empirically tested solar pump data, which are able to more accurately account for time-step response of pump flow output to variation of meteorological conditions at a given site. This way the designer of the solar water pumping system is able to predict the time-step flow output of the pump and therefore be able to size the required system components (PV array, pumping main and water storage) more economically than some previously used performance prediction models (Benghanem et al, 2018; Khan et al, 2012), and system optimization models (Hamidat and Benyoucef, 2008; Odeh et al, 2006; Bakelli et al, 2011).

2. **Problem Definition**

Solar pump manufacturers often provide laboratory measured performance characteristics of the pump such as shown on Fig.1 for a Lorentz PS21k2 CS-F42-40 solar surface pump (Chandel et al). The pump characteristic curves show the variation of the pump flow rate (Q) in response to the variation of power supplied by the PV array (P_{pv}) for a given (constant) total dynamic head (TDH). In this format, the pump data is not useful enough to enable the prediction of pump performance, given that the PV power varies with time of the day causing the flow rate to vary, which in turn cause the total dynamic head to vary depending on the material, diameter and length of the pipe line. Therefore, for accurate sizing and output prediction of the solar-powered pump-pipe system, a special empirically-driven approach is required, which takes into account the time-step variation of the response of TDH and flow rate to available solar radiation availability. The pumping system sizing and performance prediction should take into account the time-step variation of the flow-rate and total dynamic head, depending on the pumping main diameter and length being considered. Another advantage of knowing the time-step flow variation is that the water storage reservoir capacity can be determined more accurately and economically using mass balance, if the diurnal variation of water consumption is known.

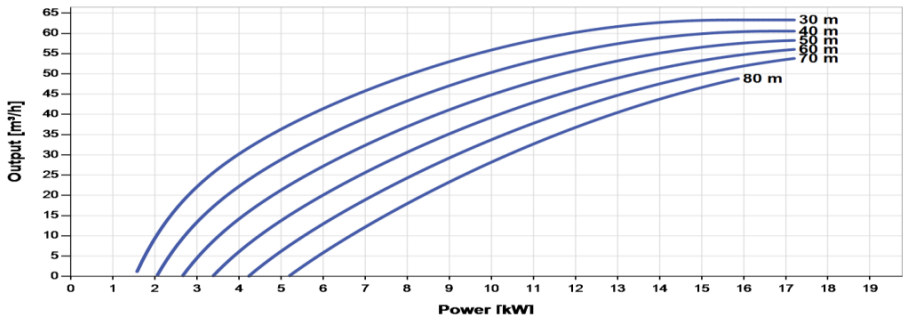

Fig 1: Pump Chart for Lorentz PS21k2 CS-F42-40 solar surface pump

The approach used in this paper is to derive empirical pump-specific functions of the time-step response of operating flow and head conditions to solar PV array power output (a function of solar irradiance and ambient temperature), for specified elevation head, pumping distance and pipe specifications. For the purpose of demonstrating the processes of this approach, a hypothetical case-study solar powered pump-pipe system, whose salient features are given on Tab.1, is studied. The system is required to pump 250 m^3/day of potable water for a rural service centre located in Zimbabwe. A Lorentz PS21k2 CS-F42-40 has been proposed using a rough selection table from a local Lorentz partner with the design flow calculated by dividing daily water requirement with location peak sunshine hours. However, the most cost-effective combination of diameter of PVC pipe, power rating of the PV array and storage size, has to be decided on. It is also required to find out if the selected pump can deliver daily water requirements. The monthly average water delivery performance of the system over the year is also required and so is the unit cost of pumping water.

Tab.1: Description of pump-pipe system

Item	Description
Location	Binga, Zimbabwe. Latitude -17.67; Longitude 27.46
Average daily water demand	250 m^3/day
Static Head	40 m
Pumping distance	2000 m
Pumping main	PVC, diameter range 90 mm; 110 mm; 125 mm to 140 mm
Pump Type	Lorentz PS21k2 CS-F42-40 solar surface pump, Maximum PV power = 21 kW

3. Solar Pump Flow-Power Functions

The proposed procedure for deriving the functions that relate the solar pump flow rate to the PV power available is as outlined below.

Step 1: Deriving Iso-Power Head-Flow (H-Q) Pump Curves

The speed of the solar pump varies as the PV power supply level (voltage) varies. Therefore, as many head-flow (*H-Q*) pump curves as there are levels of power supply can be defined. For each selected PV power supply level on Fig. 1, a pump *H-Q* curve can be defined by reading corresponding pairs of *H* and *Q* values and then fitting a best-fit curve relating *H* and *Q*. The *H-Q* relationship is of the form:

$$H_{pump} = p_2 Q^2 + p_1 Q + p_0 \qquad \text{(eq.1)}$$

In eq.1, H_{pump} [m] is the pump head at a flow rate Q [m^3/hr], p_0, p_1 and p_2 are the pump-specific regression coefficients given in Tab.2 for corresponding PV power of Fig.1 and Q [m^3/hr] is the flow rate. The H-Q curves (downward sloping curves) are plotted on Fig. 2(a).

Tab.2: H-Q regression coefficients for Lorentz PS21k2 CS-F42-40 pump

PV Power (kW)	**2**	**3.4**	**5.2**	**7**	**9**	**11**	**13**	**15**
p_2[$hr^2.m^{-5}$]	0	-0.0064	-0.0011	0.0012	-0.0027	0.0016	-0.005	0
p_1[$hr.m^{-2}$]	-1.00	1.336	-1.306	-1.562	-1.472	-2.099	-1.799	-3.064
p_0 [m]	40	59.63	79.9	99.2	115.2	146.5	160.4	223.6

Step 2: System Resistance Curve

Together with the pump *H-Q* curves, the system resistance (*TDH*) is also plotted on Fig. 2(a). The total dynamic head is given by:

$$TDH = H_0 + h_L \qquad \text{(eq. 2)}$$

The components of eq.2 i.e. TDH represents the total dynamic head of the pump, H_0 is the static head and h_L(friction and abrupt losses). For a long pipeline, the abrupt losses tend to be minor and may be neglected, and the friction loss h_f is conveniently calculated for each flow rate by the Hazen-Williams formula, Walski, 2006, as given in eq. 3.

$$V = 0.85\, C \left(\frac{D}{4}\right)^{0.63} S^{0.54} \qquad \text{(eq. 3)}$$

In eq.3, V [m/s] , is the flow velocity, D[m]is the pipe diameter of the pumping main, Q[m^3/s] is the volumetric flow rate, C is the Hazen-Williams coefficient (C = 110 for the pipes considered in this study) and S is the Slope(ratio of frictional loss to the length of the pumping main). The total dynamic head TDH is also plotted on Fig 2(a) (upward sloping curves) for a static head of 40 m and pumping distance 2000 m, and for 90, 110, 125 and 140 mm diameter PVC pipes, respectively. The total dynamic head TDH can be expressed in quadratic equation of the form:

$$TDH = H_0 + h_1 Q + h_2 Q^2 \qquad \text{(eq. 4)}$$

In eq. 4, h_1 and h_2 are system coefficients and other components have the meaning as defined above. The values of the system coefficients for the presently studied pipe diameters and pumping distances are all given on Tab.3.

Tab.3: Coefficients h_1 and h_2 for a 2000 m PVC pumping main

Pipe Diameter [mm]	**90**	**110**	**125**	**140**
h_1[hr.m^{-2}]	0.381	0.145	0.081	0.0256
h_2 [hr^2.m^{-5}]	0.0557	0.021	0.0111	0.0086

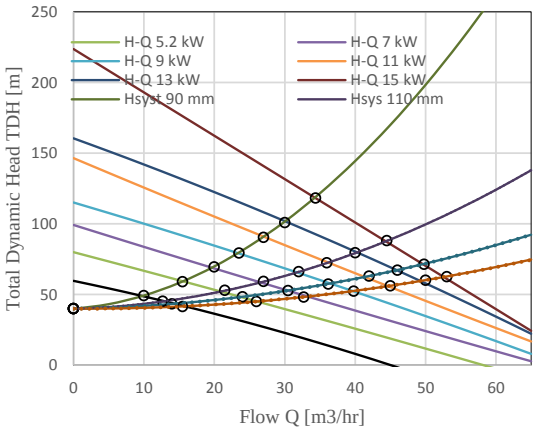

Fig.2 (a): Pump H-Q curves (downward sloping) and system curves (upward sloping) for 4 different pipe diameters.

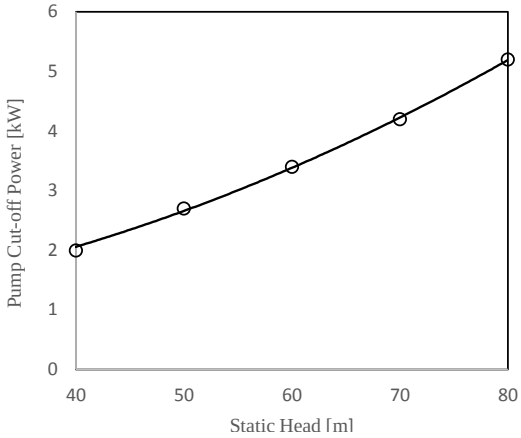

Fig.2 (b): Minimum PV power required to start the pump the (PS21k2 CS-F42-40 solar pump as a function of the static head.

Step 3: Deriving the operation flow-head-power functions of the solar pump

The intersection of the H_{pump} and TDH curves defines the operating flow rate Q_{op} and operating head TDH_{op} for the pump when connected to the respective pipe line diameters of the previously specified length. Q_{op} and TDH_{op} can be read from Fig 2 or they may be obtained analytically as the simultaneous solution of eq.1 and eq. 4 that is:

$$Q_{op} = MAX\left[0, \frac{(h_1 - p_1) \pm \sqrt{(p_1 - h_1)^2 - 4(p_2 - h_2)(p_0 - H_0)}}{2(p_2 - h_2)}\right] \qquad \text{(eq.5)}$$

$$TDH_{op} = H_0 + h_1 Q_{op} + h_2 {Q_{op}}^2 \qquad \text{(eq.6)}$$

In eq.5 and eq.6, TDH_{op} is the total dynamic head at operating point and Q_{op} is the operating flow rate. Finally, the operating flow rate Q_{op} is correlated with the PV power, P_{PV} , by pairing each Q_{op} with the corresponding P_{PV}, read from Fig 2. The $P_{PV} - Q_{op}$ correlation function is logarithmic and parametric with pipe diameter. It is of the form:

$$\begin{aligned} Q_{op} &= q_1 \ln(P_{PV}) - q_o \quad && for\ P_{PV} \geq P_{OFF} \\ Q_{op} &= 0 && for\ P_{PV} < P_{OFF} \end{aligned} \qquad \text{(eq.7)}$$

In eq.7, P_{off} is the minimum PV power which can make the pump start running. This minimum power is plotted as a function of the static head in Fig. 2(b) for the Lorentz PS21k2 CS-F42-40 solar pump. Subsequently, the wire-water operation efficiency of the solar pumping system for each PV power (a function of collected solar radiation, PV solar-electricity conversion efficiency and PV array size) is obtained as in eq. 8 with parameters as described above:

$$\eta_{pump} = \frac{\rho g Q_{op} TDH_{op}}{P_{PV}} \quad \text{(eq.8)}$$

4. Modelling the PV Power Output

As shown in the preceding section, the solar pump performance outputs Q_{op}, TDH_{op} and η_{pump_op} are driven by the PV power output P_{PV}. In turn, P_{PV} is dependent on the radiation collected on the plane of the PV array, the PV module's solar-electric conversion efficiency and its size and rated efficiency. The output power of the PV module/array of power rating P_{STC}, under arbitrary environmental conditions, can be written as:

$$P_{PV} = \frac{\eta_{PV}}{\eta_{STC}} \cdot \frac{G_T}{G_{STC}} \cdot P_{STC} \quad \text{(eq.9)}$$

In eq. 9, P_{STC} [Watts] is the rated power of the PV Array at Standard Test Conditions (STC), η_{PV} is the operating efficiency, G_T represents the irradiance measured on a tilted plane and G_{STC} is the reference irradiance. The operating efficiency is a function of temperature and is related to other constants by eq. 10

$$\eta_{PV} = F_m[1 - \beta(T_{cell} - 25)]\eta_{STC} \quad \text{(eq.10)}$$

In eq. 10, F_m is the matching factor, described as a ratio of power output of the PV array under varying operating conditions to its power output at maximum power point. A value of 0.9 is generally accepted in the PV system industry (Benghanem et al, 2018). The other parameters are β (cell efficiency temperature coefficient), and T_{cell} (cell temperature).

From eq. 10, the matching factor is described as the ratio of the power output of the PV array under operating conditions to its power output at the maximum power point. A value of 0.9 is generally accepted in PV system (Benghanem et al, 2018). The other parameters are often given on manufactures product data sheets. Since cell temperature is difficult to monitor under field operation, it is convenient to correlate it with, the ambient temperature, T_a. The standard formula for relating PV cell temperature with ambient and in-plane solar irradiance (Khan et al, 2012), which ignores the effect of wind speed on cell temperature, is given by eq. 11.

$$T_{cell} = T_a + \frac{G_T}{G_{T,NOCT}}\left(T_{C,NOCT} - T_{a,NOCT}\right) \quad \text{(eq.11)}$$

In eq. 11, $T_{C,NOCT}$ [ºC] is the nominal operating cell temperature, $T_{a,NOCT}$ at ambient temperature at NOCT and, $G_{T,NOCT}$ is the irradiance at NOCT. The irradiance incident on the plane of the PV array can be estimated by the simplified sky model justified by Collares-Pereira and Rabl, 1979.

$$G_T = G_b R_b + G_d \quad \text{(eq.12)}$$

In eq.12, G_b is the beam component of solar irradiance incident on a horizontal surface, R_b is the ratio of beam radiation on the tilted plane to that on a horizontal plane and G_d is the diffuse irradiance on the horizontal surface. Since instantaneous data of irradiance is not commonly available, it is common practice to use the average irradiance for a one hour period and evaluate R_b at the mid-point of the hour. Even the hourly solar data is rarely available, such that G_T, $G_b$and G_d have to be evaluated on monthly-average hourly basis. This is done in the following manner. Starting with the monthly-average daily irradiation on a horizontal plane, $\bar{H}_h$, the monthly-average daily diffuse irradiation, $\bar{H}_d$, is estimated from a diffuse-ratio-clearness-index correlation suitable for the given location. For Zimbabwe, the following correlation derived by Hove and Göttsche, 1999 is used.

$$\bar{H}_d = \bar{H}_h(1.0294 - 1.144\bar{K}_h) \quad for\ \bar{K}_h \geq 0.75$$

$$\bar{H}_d = 0.175\bar{H}_h \quad for\ \bar{K}_h < 0.75 \quad \text{(eq.13).}$$

In eq.13, $\bar{K}_h$ is the monthly average clearness index . The monthly-average hourly values for hourly global and diffuse radiation on a horizontal plane, $\bar{G}_h$ and $\bar{G}_d$, are then calculated by use the statistical ratios of hourly to daily radiation, r_h and r_d respectively. The ratios r_h and r_d are functions of hour angle (ω) and sunset hour angle (ω_s), and their expression have been given by Collares-Pereira and Rabl, 1979:

$$r_h = \bar{G}_h / \bar{H}_h \text{ and } r_d = \bar{G}_d / \bar{H}_d \quad \text{(eq.14)}$$

Monthly average global radiation data for locations in Zimbabwe can be extracted from the $0.5° \times 0.5°(longitude \times latitude)$ grid database developed by Hove et al, (2014), by applying the technique of bilinear interpolation. Data for ambient temperature is readily available online as monthly average minimum and maximum values, e.g. from the online source (https://en.climate-data.org/africa/zimbabwe/matabeleland-north/binga-29995/). Hourly ambient temperature was generated from monthly average minimum and maximum ambient temperature using the statistical model developed in Wit, 1978. Tab. 4 lists the monthly average ambient temperature at longitude 27.6° and latitude -*17.67*°. The tilt factor, which is the ratio of global radiation on the tilted plane to that on the horizontal surface, is also listed on Tab.4 for an optimal fixed collector tilt of 23° (about latitude + 5°).

Tab.4: Monthly Average Climatic Data for Binga, Zimbabwe, longitude 27.46° & latitude -17.67°. Source: Hove and Göttsche, 1999 for solar radiation data and (En.climate-data.org) for ambient temperature data.

Month	Min. Temperature (°C)	Max. Temperature (°C)	Global Horizontal Irradiation (Wh/m²/day)	Diffuse Horizontal Irradiation (Wh/m²/day)	Tilt Factor (at 23° tilt)
January	20.6	30.6	6514	2495	0.90
February	20.2	30.1	6517	2441	0.95
March	19.6	31.5	6526	1977	1.01
April	17.9	31.6	6284	1434	1.12
May	14.2	30.7	5798	1015	1.24
June	11.6	28.6	5162	1010	1.27
July	11.4	28.9	5583	997	1.28
August	14	31.1	6215	1123	1.17
September	18.2	34.4	6710	1597	1.05
October	21.6	36.5	7131	1944	0.96
November	21.6	33.9	6976	2291	0.91
December	20.9	31.3	6797	2437	0.89

5. Sizing of System Components

5.1 Size of PV Array

The size of PV array is obtained by iteratively varying the PV power (P_{STC}) and use eq.7 to determine the hourly PV power. With hourly values, the flow rate for each hour is then determined from the flow-power functions typified by eq.9 which when integrated numerically over time gives the daily water volume delivered by the pump. The PV array power is varied until the monthly-average daily volume of water delivered is just equal to the daily water demand for the least productive month of the year. Tab.5 demonstrates how the PV array size is determined when the solar pump is connected with a 140 mm diameter pipe of 2000 m length. The PV array power is altered in small steps until the required daily pumped volume of water of 250 m^3 is obtained. The simulation is done for the month of January, which is the least productive in terms of average daily water yield over the year at Binga. The last row on Tab. 5 shows the monthly average sums or averages (in parenthesis) of the solar pumping system performance parameters.

The average PV array efficiency $\bar{\eta}_{PV}$ is obtained as the numerical integral of the hourly PV power over the day divided by the integral of hourly irradiance multiplied by the PV array area. Similarly the average pump efficiency $\bar{\eta}_{pump\_op}$ is the sum of the hydraulic power output $\sum \rho g Q_{op} H_{op}$ divided by $\sum P_{PV}$. The overall average solar-to- water efficiency $\bar{\eta}_{overall}$ is then $\bar{\eta}_{PV} \times \bar{\eta}_{pump\_op}$. In this particular case, where the pump is connected with a 125 mm diameter pipe, the required PV array power (that which is required to yield the daily water demand of 250 m^3) is 12720 Watts and the average overall efficiency is 0.060. The process shown on Tab. 5 was repeated for the rest of pumping main pipe diameters, and for all the months of the year.

5.1 Selection of pipe diameter

In order to make an objective selection of the pipe size to use in the solar-powered pump-pipe system, it is necessary to define an appropriate objective-function metric to use for comparison. The comparison metric used in this paper is

the *unit cost of pumping*. The unit cost of pumping is calculated as the annualized cost of the sum of capital costs of the solar PV array; the pipe line and the pump-motor-controller unit, plus the annual maintenance costs, all divided by the annual volume of water pumped. For each capital asset of the pumping system, the annualized cost is calculated from eq.15, for a discount rate of r% and an asset life of n years.

$$c_{pumping} = C_{capex} \times \frac{r}{1-(1+r)^{-n}} + C_M \qquad \text{(eq.15)}$$

Tab.5: Computation of Solar Pump Performance and Determination of Required PV Array Size

DESIGN DATA										
Location and Climate Location: Longitude 27.46; Latitude -17.67 Design Month: January Global Solar Radiation: 6.62 kWh/m^2/day Minimum Ambient Temperature: 20.6℃ Maximum Ambient Temperature: 30.6℃			*Pipe System & Resistance* Static Head: 40 m Pipe diameter: 125 mm Pumping Main Length: 2000 m h_1:0.081 h_2 : 0.0111			*PV Array Parameters* η_{STC}: 15.5% β: 0.0041/ ℃ T_{NOCT}: 46℃ P_{STC}: **12720 W**		*Pump Flow-Power Coefficients* q = 24.35 q_0 = -16.51		
Solar Time [Hour]	G_T [Wh/m2] Eqn. (12)	T_a [℃] Table 5	T_c ℃ Eqn. (11)	η_{PV}/η_{STC} Eqn. (10)	P_{PV} [Watts] Eqn. (9)	Q_{op} [m^3/hr] Eqn. (7)	*THD* [m] Eqn. (6)	$\rho g Q_{op} T DH$ [Watts]	η_{pump} Eqn. (8)	$\eta_{overall}$ ($\eta_{pump} \times \eta_{PV}$)
6.5	95	20.7	23.8	0.90	1096	0.000	40.0	0	0.0%	0.0%
7.5	259	21.3	29.7	0.88	2910	9.500	41.8	1081	37.2%	5.1%
8.5	436	22.6	36.7	0.86	4755	21.459	46.8	2740	57.6%	7.6%
9.5	602	24.2	43.8	0.83	6363	28.550	51.4	3996	62.8%	8.1%
10.5	731	26.0	49.8	0.81	7517	32.607	54.4	4837	64.4%	8.1%
11.5	801	27.8	53.8	0.79	8087	34.388	55.9	5239	64.8%	8.0%
12.5	801	29.3	55.3	0.79	8032	34.221	55.8	5201	64.8%	7.9%
13.5	731	30.3	54.0	0.79	7372	32.132	54.1	4734	64.2%	7.9%
14.5	602	30.6	50.2	0.81	6182	27.848	50.9	3860	62.4%	7.8%
15.5	436	30.3	44.4	0.83	4598	20.637	46.4	2609	56.8%	7.3%
16.5	259	29.3	37.7	0.85	2813	8.676	41.5	982	34.9%	4.6%
17.5	95	27.8	30.9	0.88	1064	0.000	40.0	0	0.0%	0.0%
Sum or (average)	**5850**	**(26.7)**	**(42.5)**	**(0.84)**	**62163**	**250.0**	**(48.25)**	**35279**	**(47%)**	**(6.0%)**

In eq.15, r is the discount rate [%], n is the life span of project [years], C_M represents the maintenance cost, C_{capex} is the capital cost of the asset and $C_{pumping}$ *is the* cost of pumping[\$/m^3]. The annual volume of water pumped for each PV-pump-pipe design is obtained by computing the monthly-average daily volume pumped as done on Tab.5, multiply it by the number of days in each month and then summing the monthly delivered volumes over the year. The PV-pump-pipe design resulting in the lowest cost of pumping calculated as above should be the rational design choice for the solar pump system. The choice of the PV-pump-pipe design is not obvious since a larger diameter pipe (large pipe costs) requires a smaller PV array size (small PV array costs). In principle, the size of the pump itself may also vary for different pipe diameters used to perform a given pumping duty, therefore changing the cost structure of the PV-pump-pipe system.

5.2 Sizing the water storage capacity required for the solar pumping system

The water storage capacity required for the solar pumping scheme is ordinarily determined by multiplying the average daily water demand by the days of autonomy (usually 2 to 5 days) required to cater for long cloudy periods. However, due to the nature of the method used in this study, which allows the monthly-average hourly variation of pumped flow to be determined, the storage capacity may be determined in a different and more economical way.

Assuming, for instance, a diurnal water draw profile given in Blokker, 2011, and the hourly solar pump flow on Tab. 5, the demand-supply hourly variation is plotted on Fig.3(a). The corresponding cumulative water demand and supply

can then also be plotted as shown on Fig.3(b). The quantity of water required to be stored in the reservoir for equalising or balancing fluctuating demand against fluctuating supply (balancing storage) can be worked out by the mass curve method (Khatib, 2010). It is calculated from Fig.3(b) as the sum of "maximum deficit" plus "maximum surplus". In the present case, the required balancing storage is 46 + (250-177) = 119 m^3, or 48% of the daily demand. To obtain the required storage 25% of balancing storage capacity should be added to cater for system breakdowns. This still gives only 60% of the daily water, demand before the days of autonomy multiplier is factored in.

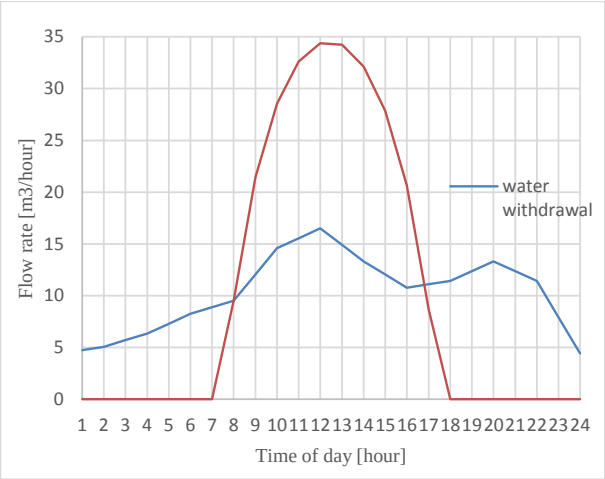

Fig.3 (a): Hourly net-flows of the Solar Powered Scheme

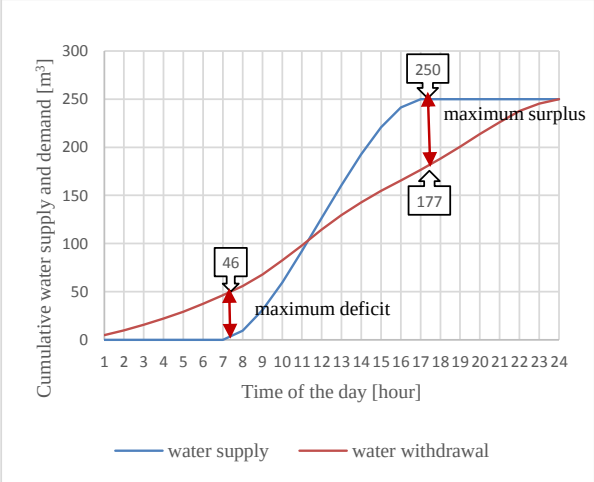

Fig.3 (b): Mass Balance curve for the Solar Powered Scheme

6. Results and Discussion

The results for the proposed procedure for PV-pump-pipe design are presented and discussed in this section.

6.1. Flow-Power Functions

As mentioned in Section 3 the flow-power functions within the operating range of the solar pump system is of the form $Q_{op} = q_1 ln(P_{PV}) - q_0$ (eq. 7). The coefficients q_0 and q_1 of eq.7 are given on Tab. 6 and plotted on Fig. 4, for the case-study system- a system pumping through 2000 m long 90, 110, 125 or 140 mm diameter PVC pipes and against a static head of 40 m.

Tab. 6: Coefficients of the flow-power function (eq.7)) for the Lorentz PS21k2 CS-F42-40 pump connected to 2000 m PVC pipe length of different diameters and for 40 m static head

Pipe diameter [mm]	**90**	**110**	**125**	**140**
q_0	-10.90	-14.17	-16.51	-17.43
q_1	16.10	21.27	24.35	26.10

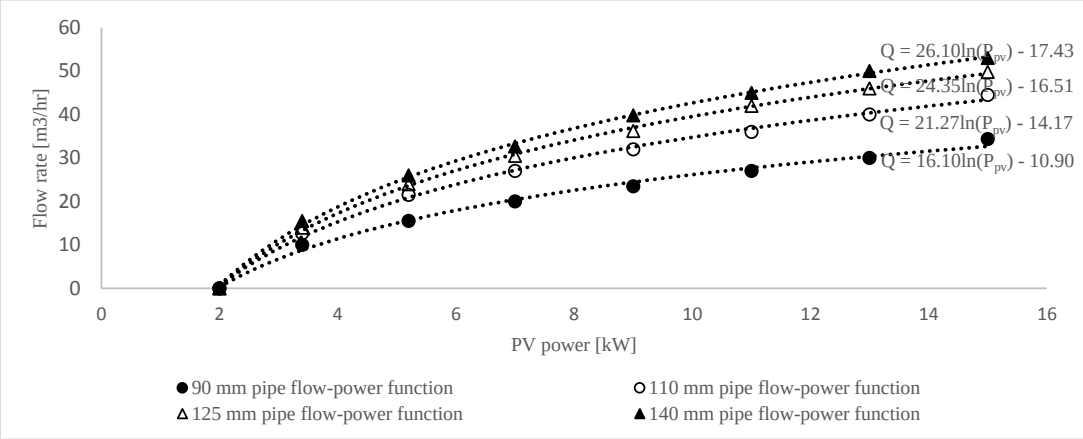

Fig. 4: Flow rate to PV-power response functions for different pipe diameters

6.2. System efficiencies

The modelled hourly variation of the solar pump system efficiencies for system with 125 mm diameter pipe and 12720 Watts PV array power are shown on Fig. 5 on the average day of January. The PV efficiency of eq.10 is higher in the early morning and late afternoon, when the ambient and cell temperatures are low, than in the mid-day hours when ambient and cell temperatures are higher. On the other hand, the pump efficiency is highest during the mid-day hours. The overall system efficiency is the product of the PV efficiency and pump efficiency. The overall solar pumping system efficiency increases fairly rapidly from zero in the early morning, peaks in the mid-morning (when the product of PV efficiency and pump efficiency is highest) and then reduces gradually over most of the day, before falling rapidly to zero in the late afternoon.

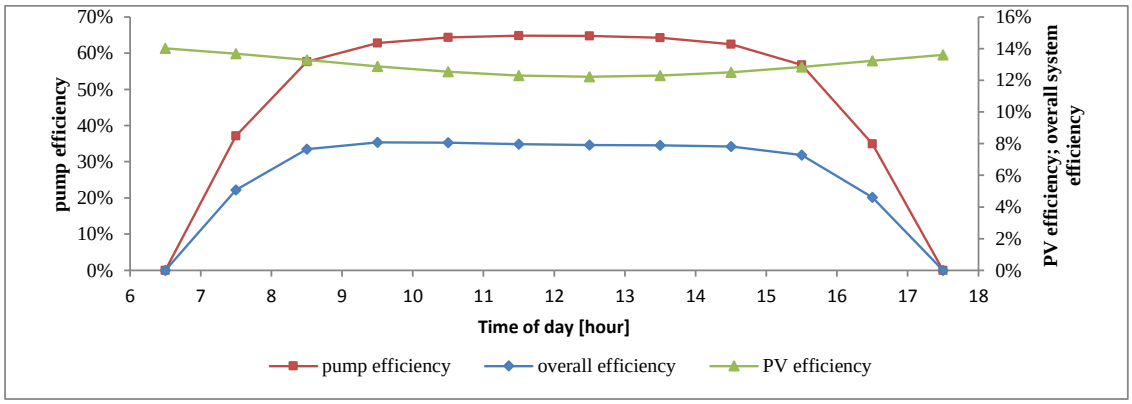

Fig.5: Hourly variation of PV efficiency, pump efficiency and overall system efficiency for the month of January (lowest pump yield) at Binga, Zimbabwe.

6.3. Designed Systems

The relationship between the required PV array power and the diameter of the pipe employed in the solar pump-pipe system is shown on Fig. 6(a). The PV array power required to deliver the daily average water demand (250 m^3/day) in the least productive month reduces as shown on Fig. 6(a) as the pipe diameter is increased. The required PV array power almost halves as the pipe diameter is increased from 90 mm to 140 mm. Although each of the systems is designed to deliver 250 m^3/day in January (the least productive month), their cost structures are different, since they used different PV array and pipe sizes. Further, they deliver slightly different annual volumes of water as shown on

Fig. 6(b). For an instructive comparison of the systems' cost effectiveness, the unit cost of pumping is compared. This is shown of Tab. 7. As shown on Tab. 7, the system with the least unit cost of pumping, which is the preferred system, is the one that combines a 125 mm diameter pumping main with a 12720 Watt PV array. The unit cost of pumping for this system is 5.22 cents per m^3 of water pumped.

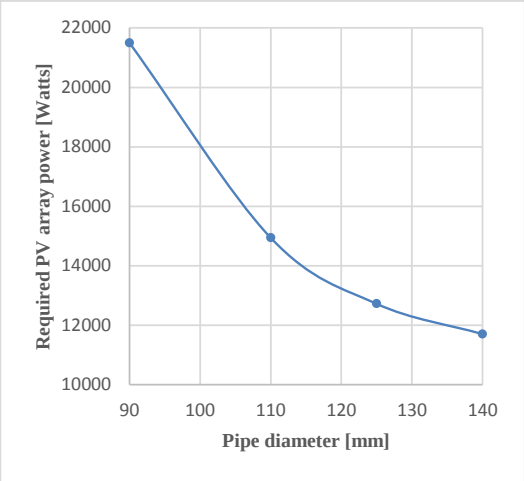

Fig.6 (a): Required PV array variation with pipe diameter for the study solar pump at 40 m static head and length of 2000m.

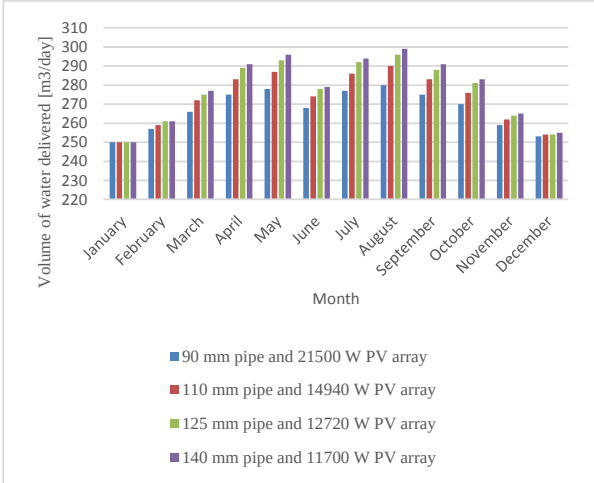

Fig.6 (b): Monthly variation of daily-water delivery for different pump-piping systems

Tab.7: Variation of unit cost of pumping for PV systems designed to deliver a minimum of 250 m^3/day water at static head 40 m and pumping distance 2000 m.

Item	**90 mm diameter pipe**	**110 mm diameter pipe**	**125 mm diameter pipe**	**140 mm diameter pipe**
Pump cost [$]	13,700	13,700	13,700	13,700
Pipe cost per m [$/m]	3.00	3.65	4.62	5.81
Pipe capital cost for 2000 m [$]	6,000	7,300	9,240	11,620
Required PV power [Watts]	21500	14940	12720	11700
PV cost/Watt [$/Watt]	1.00	1.00	1.00	1.00
PV capital cost [$]	21500	14940	12720	11700
Pipe O & M (3%) [$/annum]	120	146	184.8	232.4
PV O & M (2%) [$/annum]	430	298.8	254.4	234
Pump O & M (10%) [$/annum]	685	685	685	685
Pump lifespan [years]	15	15	15	15
PV lifespan [years]	25	25	25	25
Pipe lifespan [years]	40	40	40	40
Annualized cost at 10% discount rate [$]	6018	5323	5272	5430
Annual water pumped water [m3]	97526	99590	100958	101566
Cost of pumping [$/m3]	6.17	5.35	5.22	5.35

7. Comparing Study Method with Simple Sizing Method

The simple procedure often used for sizing solar pumping systems is compared below with the method used in this

study. Starting with the known daily water demand (250 m^3/day), the required pump flow rate is obtained by dividing the daily demand by the effective peak sunshine hours, for the month receiving the least tilted-radiation. From Tab.4, the least tilted-plane irradiation is received for the month of January. The monthly average global horizontal irradiation is 6.514 kWh/m^2/day and the tilt factor is 0.9, resulting in global irradiation on the tilted plane of 5.859 kWh/m^2/day. Now, only part of this radiation is available above the critical irradiance for pump start-up. This fraction is estimated here to be 0.95. Therefore, the effective monthly average irradiation available for pump operation is 0.95 x 5.859, which is 5.566 kWh/m^2/day or 5.566 peak sunshine hours. Therefore, the required flow-rate of the pump is 250 m^3 divided by 5.566 hours, equals about 45 m^3/hr.

Using the 125 mm diameter pipe selected in section 8.3, the Hazen-Williams formula yields a frictional head loss of about 26 m for a flow-rate of 45 m^3/hr over a distance of 2000 m. Therefore, the total dynamic head for a static head of 40 m is 66 m. From the pump characteristic curve of Fig.1, the nominal PV array power required to deliver 45 m^3/hr at 66 m head is 12.6 kW. To be comparable with the PV array power calculated by our study method, a de-rating factor that includes both PV module mismatch factor and temperature de-rating, as done in eq.10, has to be incorporated. A cell temperature of about 52°, which, for example in Tab.5, is the average cell temperature between 9 am and 3 pm (when the bulk of the solar energy is produced), eq.10 yields a temperature de-rating factor, η_{PV}/η_{STC}, of about 0.80.Therefore, the PV array power that would have been prescribed using the simple design method is 12.6/0.79 or 15.75 kW.

Compared with the PV array power prescribed by the study method (12.72 kW), the PV array size prescribed by the simple sizing method is 24% larger. The reason for this discrepancy is that the simple sizing method uses a single average flow-rate calculated based on average peak sunshine hours, resulting in a commensurate total dynamic head, which is higher than the variable flow-rates and total dynamic head actually obtaining during pump operation. Another difference is the balancing storage size, which can be calculated using hourly mass balance with the study method, but is assumed equal to daily water demand with the simplified method. As shown in section 5.3, the storage capacity sized using the study method is much smaller (50% smaller) compared to that obtained by the simple sizing method.

8. Conclusion

A method that can be used to optimally size and predict performance of a solar pumping system was demonstrated for a solar pumping system located in Zimbabwe. For a given pump, the components of the solar pumping system that need to be carefully sized are the PV array, the pipe diameter and the storage tank. The method considers comprehensively the time-step variation of solar irradiance and its effect on the pump system flow-rate and total dynamic head. For a given pumping main pipe diameter, the PV array power that can deliver a required daily volume of water, under the mentioned dynamic variation of pump operating parameters, can be selected by trial and error. Especially for fairly long pumping mains, the PV array power required to deliver a specified daily volume of water reduces significantly as the pumping main pipe diameter is increased. Depending on the relative specific costs of PV array and pipe, an economically optimum (least unit cost of pumping) combination of these two system components, which delivers the desired daily volume of water, can be arrived at.

The method is a significant improvement to the commonly used simplified approach of sizing solar pumping systems as it can result in significantly reduced system size. Using the study method, it is also more possible to predict the monthly average hourly variation of delivered water as well as its month-to-month variation. With knowledge of the average hourly variation of volume of water delivered coupled with information on the diurnal water demand, it is possible to more accurately estimate the required balancing water storage size for the solar pumping scheme, which turns out to be much smaller than the ordinarily assumed storage capacity.

9. References

[1] Bakelli. Y, Hadj, A. and Azoui, C. (2011), Optimal sizing of photovoltaic pumping system with water tank storage using LPSP concept, Solar Energy, Volume 85, Issue 2, 288-294.

[2] Benghanem, M., Daffallah, K. O., Almohammedi, A. (2018), Estimation of daily flow rate of photovoltaic

water pumping systems using solar radiation data, Results in Physics, Volume 8, 949-954.
[3] Blokker, M. (2011), Stochastic water demand modelling, London: IWA Pub., pp. 37.
[4] Chandel, S. S., Nagaraju Naik M. and Chandel R. (2015), Review of solar photovoltaic water pumping system technology for irrigation and community drinking water supplies, Renewable and Sustainable Energy Reviews, Volume 49, 1084-1099.
[5] Collares-Pereira, M. and Rabl, A. (1979), The average distribution of solar radiation-Correlations between diffuse and hemispherical and between daily and hourly insolation values, Solar Energy, 22, 155-164.
[6] En.climate-data.org. (2017), Climate data for cities worldwide - Climate-Data.org. [online] Available at: https://en.climate-data.org/africa/zimbabwe/matabeleland-north/binga-29995/, [Accessed 31 Dec. 2017].
[7] Foster, R. and Cota, A. (2014). Solar Water Pumping Advances and Comparative Economics, Energy Procedia, 57, 1431-1436.
[8] Hamidat A, Benyoucef B. (2008), Mathematic models of photovoltaic motor-pump systems. Renewable Energy, Volume 33:933–4.
[9] Hove T. and Göttsche J. (1999), Mapping global, diffuse and beam solar radiation over Zimbabwe. Renewable Energy 18 (4), 535-556.
[10] Hove, T., Manyumbu, E. and Rukweza, G. (2014), Developing an improved global solar radiation map for Zimbabwe through correlating long-term ground- and satellite-based monthly clearness index values. *Renewable Energy*, 63, 687-697.
[11] Khan MTA, Ahmed MR, Ahmed SI, Khan SI (2012), Design and Performance analysis of water pumping using solar PV. In: Proceedings of the international conference of developments in renewable energy technology (ICDRET).
[12] Khatib, T. (2010), Deign of Photovoltaic Water Pumping Systems at Minimum Cost for Palestine: A Review. *Journal of Applied Sciences*, 10(22), 2773-2784.
[13] Klemeš, V. (1979), Storage mass-curve analysis in a systems-analytic perspective, *Water Resources Research*, 15(2), 359-370.
[14] Odeh, I., Yohanis, Y.G. and Norton, B. (2006), Influence of pumping head, insolation and PV array size on PV water pumping system performance, Solar Energy, Volume 80, Issue 1, 51-64.
[15] Schwingshackl, C., Petitta, M., Wagner, J., Belluardo, G., Moser, D., Castelli, M., Zebisch, M. and Tetzlaff, A. (2013), Wind Effect on PV Module Temperature: Analysis of Different Techniques for an Accurate Estimation. *Energy Procedia*, 40, 77-86.
[16] Walski, Thomas M. (March 2006), A history of water distribution, Journal-American Water Works Association, ***98*** *(3): 110–121*, p. 112.
[17] Wit, C. (1978), Simulation of assimilation, respiration and transpiration of crops, Wageningen: Centre for Agricultural Publishing and Documentation, pp.148.